Deployment of the Hobby-Eberly Telescope Wide Field Upgrade[†]

Gary J. Hill[a,b‡], Niv Drory[a], John M. Good[a], Hanshin Lee[a], Brian L. Vattiat[a], Herman Kriel[a,c], Jason Ramsey[a], Randy Bryant[c], Linda Elliot[a], Jim Fowler[c], Marco Häuser[d], Martin Landiau[a], Ron Leck[a], Stephen Odewahn[c], Dave Perry[a], Richard Savage[a], Emily Schroeder Mrozinski[c], Matthew Shetrone[c], D.L. DePoy[d], Travis Prochaska[d], J.L. Marshall[d], George Damm[c], Karl Gebhardt[b], Phillip J. MacQueen[a], Jerry Martin[c], Taft Armandroff[a,b], Lawrence W. Ramsey[f]

[a] McDonald Observatory, [b] Department of Astronomy, [c] Hobby-Eberly Telescope, University of Texas at Austin, 2515 Speedway, C1402, Austin, TX 78712, USA
[d] Universitäts-Sternwarte München, Scheinerstr. 1, 81679 München, Germany
[e] Department of Physics and Astronomy, Texas A&M University, 4242 TAMU, College Station, TX 77843, USA
[f] Department of Astronomy, Pennsylvania State University, 516 Davey Lab, University Park, PA 16802, USA

ABSTRACT

The Hobby-Eberly Telescope (HET) is an innovative large telescope, located in West Texas at the McDonald Observatory. The HET operates with a fixed segmented primary and has a tracker, which moves the four-mirror corrector and prime focus instrument package to track the sidereal and non-sidereal motions of objects. We have completed a major multi-year upgrade of the HET that has substantially increased the pupil size to 10 meters and the field of view to 22 arcminutes by replacing the corrector, tracker, and prime focus instrument package. The new wide field HET will feed the revolutionary integral field spectrograph called VIRUS, in support of the Hobby-Eberly Telescope Dark Energy Experiment (HETDEX[§]), a new low resolution spectrograph (LRS2), an upgraded high resolution spectrograph (HRS2), and later the Habitable Zone Planet Finder (HPF). The upgrade is being commissioned and this paper discusses the completion of the installation, the commissioning process and the performance of the new HET.

Keywords: **Keywords:** Hobby-Eberly Telescope, HET, HETDEX, wide field corrector, tracker, spectrographs: VIRUS, integral field

1. INTRODUCTION

The HET[1-6] (Fig. 1) is an innovative telescope designed to be cost-effective for large surveys. It has an 11 m hexagonal-shaped spherical primary mirror made of 91 1-m hexagonal segments that sits at a fixed zenith angle of 35°. HET is the basis for the Southern African Large Telescope (SALT)[7]. It can be moved in azimuth to access about 70% of the sky visible at McDonald Observatory (δ = -10.3° to +71.6°). The pupil was originally 9.2 m in diameter, set by the spherical aberration corrector design, and sweeps over the primary mirror as the x-y tracker follows objects for between 50 minutes (in the south at δ = -10.0°) and 2.8 hours (in the north at δ = +67.2°). The maximum time on target per night is 5 hours and occurs at +63°. The HET primary mirror has a radius of curvature of 26164 mm. The original 4-mirror double-Gregorian type corrector had a 4 arcmin (50 mm) diameter science field of view. Detailed descriptions of the original HET and its commissioning can be found in refs 1-3.

[†] The Hobby – Eberly Telescope is operated by McDonald Observatory on behalf of the University of Texas at Austin, Pennsylvania State University, Ludwig-Maximillians-Universität München, and Georg-August-Universität, Göttingen
[‡] G.J.H.: E-mail: hill@astro.as.utexas.edu
[§] http://hetdex.org/

Ground-based and Airborne Telescopes VI, edited by Helen J. Hall, Roberto Gilmozzi, Heather K. Marshall,
Proc. of SPIE Vol. 9906, 990606 · © 2016 SPIE · CCC code: 0277-786X/16/$18 · doi: 10.1117/12.2231063

The HET was envisioned originally as a spectroscopic survey telescope, able to efficiently survey objects over wide areas of sky. While the telescope has been very successful at observing large samples of objects such as QSOs and extrasolar planets spread over the sky with surface densities of around one per 10 sq. degrees, the HET design coupled with the limited field of view of the original corrector hampers programs where objects have higher sky densities. In seeking a strong niche for the HET going forward, the HET field of view will be increased from 4′ to 22′ so that it can accommodate the Visible Integral-field Replicable Unit Spectrograph (VIRUS)[8-11], an innovative, highly multiplexed spectrograph that will place 35,000 fibers on sky simultaneously and open up the emission-line universe to systematic surveys for the first time, uncovering populations of objects selected by their line emission rather than by their continuum emission properties.

The primary motivation for the HET wide field upgrade (WFU) and VIRUS is to execute the Hobby-Eberly Telescope Dark Energy Experiment (HETDEX[12]), which will map the spatial distribution of about 0.8 million Lyα emitting galaxies (LAEs) with redshifts $1.9 < z < 3.5$ over a 420 sq. deg. area (9 Gpc^3) in the north Galactic cap. This dataset will constrain the expansion history of the Universe to 1% and provide significant constraints on the evolution of dark energy. The requirement to survey large areas of sky with VIRUS plus the need to acquire wavefront sensing stars to provide full feedback on the tracker position led us to design an ambitious new corrector employing meter-scale aspheric mirrors and covering a 22-arcmin diameter field of view.

The WFU deploys the wide field corrector (WFC[13-15]), a new tracker[16,17], a new prime focus instrument package (PFIP[18,19]), and new metrology systems[18-23]. The metrology systems are intended to provide closed-loop feedback on all axes of motion and the optical configuration of the telescope. They include guiding, wavefront sensing, payload tilt sensing, and a distance measuring interferometer (DMI). Together they control the alignment of the WFC to the primary mirror as well as providing feedback on the temperature-dependent radius of curvature of the primary mirror, which is on a steel truss.

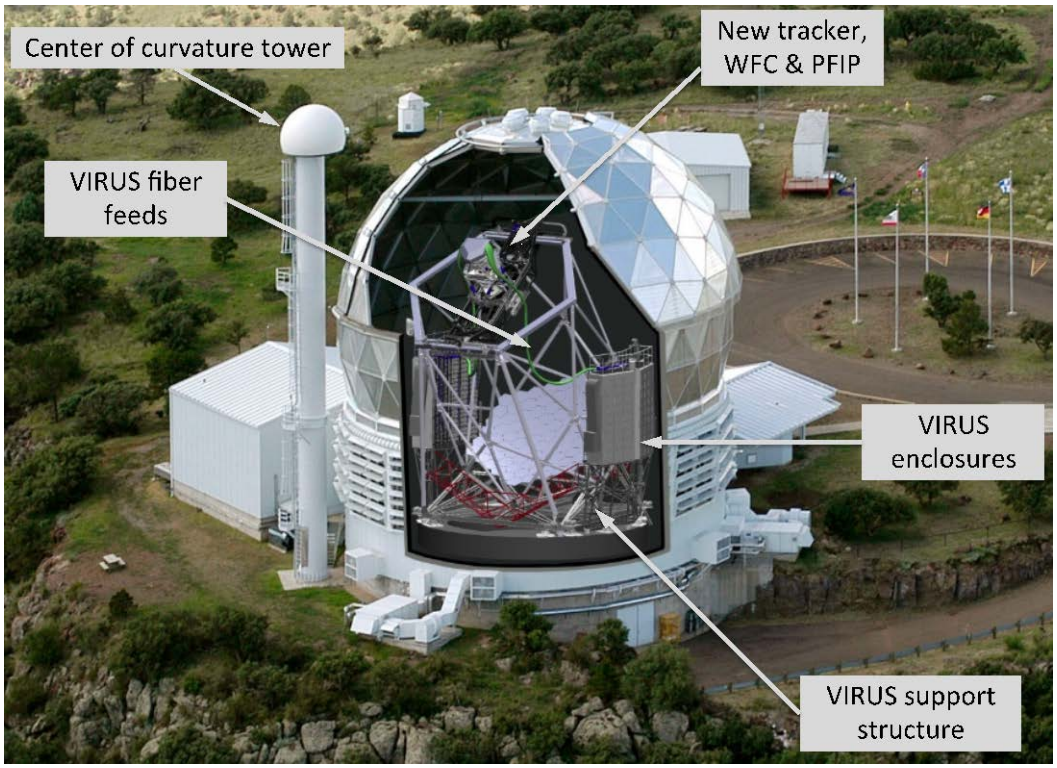

Figure 1. The layout of the HET with rendering of the WFU and VIRUS superimposed. The WFU replaces the top end of the HET with a new tracker, wide field corrector (WFC) and prime focus instrument package (PFIP). The highly replicated VIRUS spectrograph units are housed in two enclosures either side of the structure, which are mounted on the VIRUS support structure, and fed by 35,000 fibers from the prime focus.

2. TELESCOPE CONFIGURATION

The basic configuration of the HET is unchanged in the upgrade, but the new tracker has a much higher payload of 3 tonnes to accommodate the new WFC and PFIP. VIRUS is fiber-fed which allows the mass of the spectrographs to be carried in two enclosures one on each side of the telescope (Fig. 1). Each enclosure can support 40 pairs of spectrographs (VIRUS units have two spectrograph channels, and disperse the light from an IFU with 448 fibers), there is capacity for a total of 80 units. VIRUS has 78 units (156 spectrographs with coverage per observation of 60 sq. arcminutes. The other enclosure slots house the two units of the new Low Resolution Spectrograph (LRS2[23]). Figures 1 and 2 show CAD renderings of the telescope post upgrade and identify the major components.

The key configuration change to the facility is the addition of the enclosures and support structure for VIRUS (Figure 1). The location of the spectrograph enclosures was constrained by many factors, including:

- Desire to maximize throughput (especially in the UV) by minimizing the length of the fiber feeds
- Minimize the mechanical stress on the fiber feeds
- Maintain adequate man-lift access to the telescope's interior structure. This is particularly important because the mirror segments are cleaned with CO_2 several times a week, and the individual mirror segments are removed and recoated on a regular basis.
- Prevent wind-induced motion of the spectrograph enclosures (which have an effective wind sail area on the order of 50 m^2) from shaking the telescope structure and causing image degradation
- Minimize complexity, weight, and cost of the structure, which supports the spectrograph enclosures

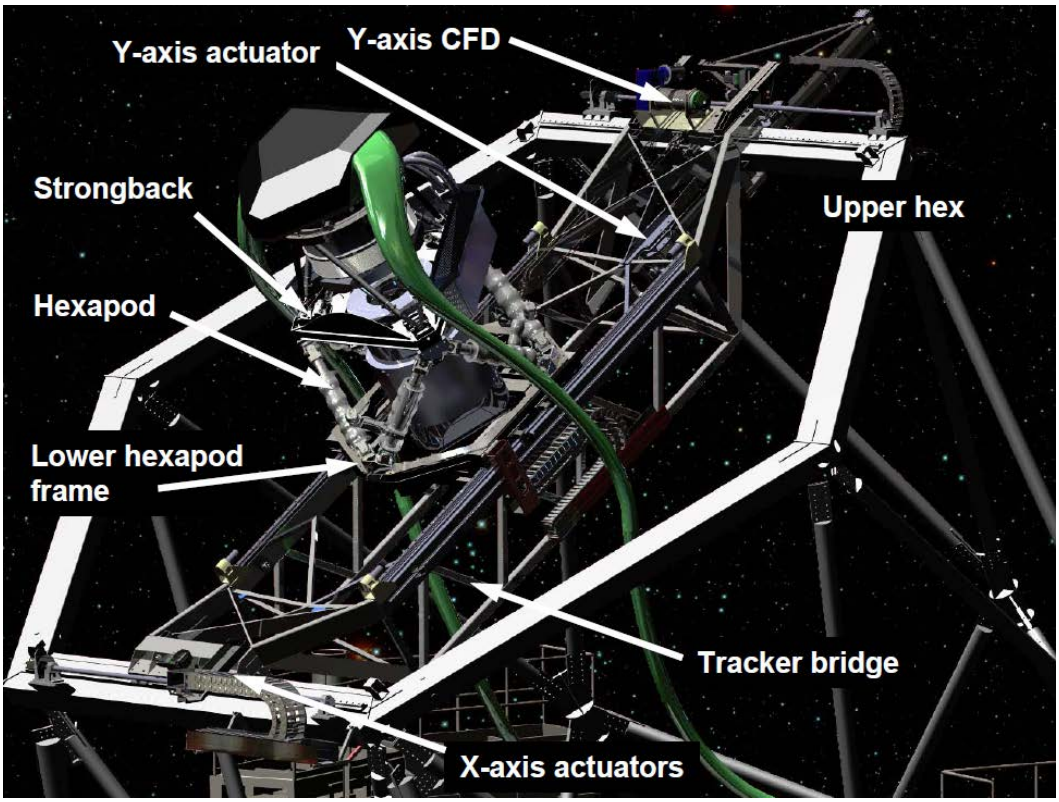

Figure 2. Close up view of the top of the telescope post WFU with key components indicated. New features compared to the old HET tracker are the center drive on the y-axis and the addition of the y-axis constant force drive (CFD).

The final enclosure locations were a compromise that was strongly influenced by the need to maintain man lift access to the primary mirror. The VIRUS Support Structure[24] is a complex weldment that interleaves with the main telescope structure without applying loads to it that could couple wind induced vibration from the enclosures to the telescope. It rides on separate air-bearings that lift it during changes in telescope azimuth, and is pulled round by the main azimuth drive. The enclosures are large clean rooms with air circulation and heat extraction to remove heat from the VIRUS

controllers and ensure that the skin temperature of the enclosures remains close to ambient to ensure they do not impact the dome seeing.

3. TRACKER

A new tracker is needed to accommodate the size and five-fold weight increase of the new WFC and PFIP. It represents a third generation evolution of the trackers for HET and SALT, and is in essence a precision six-axis stage (Figs. 2, 3). The tracker bridge spans the upper hexagon of the telescope structure, moving on two x-axis stages with skew sensing in case they become misaligned. A carriage moves up and down in the y-axis, and supports the hexapod that provides the fine adjustment in the other degrees of freedom. The total volume of motion is about 7x7x4 m^3, and the required accuracy is on the order of 10 μm and 4 arcseconds in tilt.

The tracker was built by the Center for Electro-Mechanics (CEM) and McDonald Observatory (MDO) at the University of Texas at Austin[16,17,25-28]. After integration and testing was finished it underwent a test plan that was completed in mid 2013[16,17]. Testing was based on using a laser tracker (LT, model API T3-40 with DMI) to map out deflections in six degrees of freedom relative to an ideal spherical surface, surrogate for the HET primary mirror focal surface. The accuracy of the measurements was below 100 microns, well within the capture range of metrology systems to be deployed with the upgrade. We demonstrated that the deviations from a sphere were well-behaved and had residuals better than 100 microns, and that we could adjust the working point of the track axially. The latter is required to match the tracking sphere to the point where the WFC can be tilted without moving the image (the stationary-image rotation point or SIRP). We further verified that guide offsets could be executed within the required time and to better than the required accuracy. Following a Readiness Review in July 2013 for the upgrade, the new tracker was packed and shipped in stages as the old HET tracker was dismantled and the structure prepared for the installation of the new tracker by welding on stiffening sections on the upper and lower beams of the top-hexagon. The upper and lower X-axes were installed in late 2013. The tracker bridge was the last major item to be shipped and installed over 2 days in February 2014 with a large external crane. The hexapod system was installed and the tracker commissioned in mid 2014.

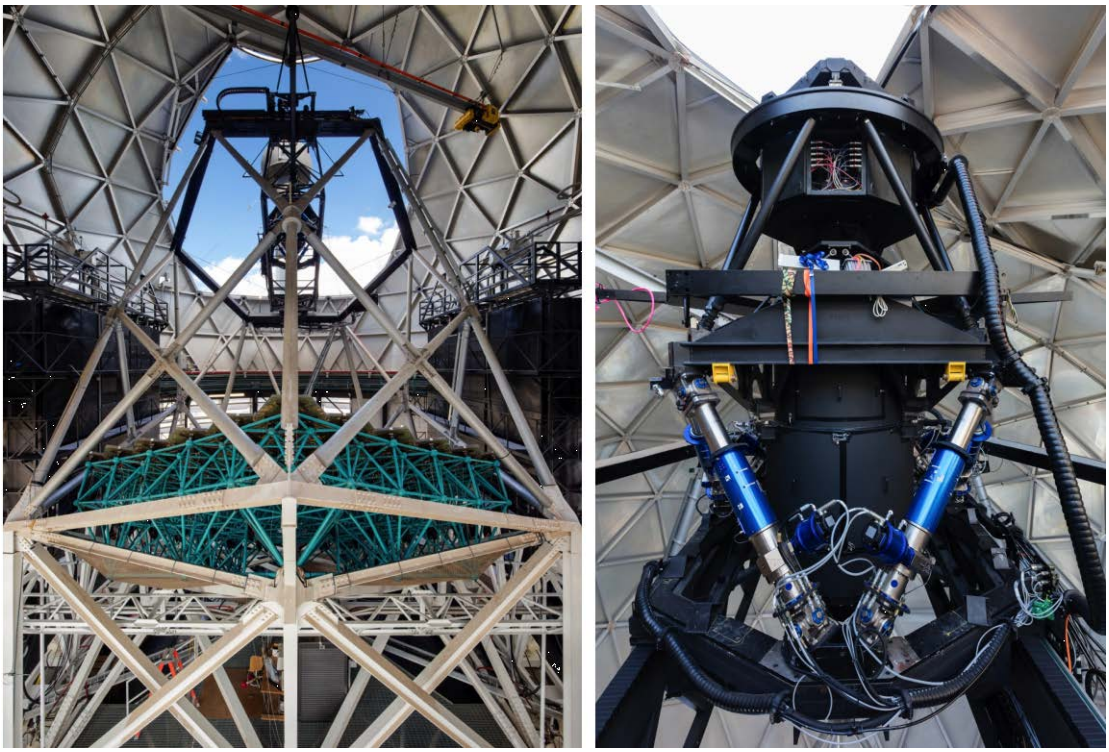

Figure 3: Images of completed HET upgrade. Left – view from behind primary mirror, showing the new tracker centered in the upper hexagon of the telescope structure, and showing the VIRUS enclosures either side of the telescope. Right – view of the WFC and PFIP. The hexapod struts that orient the WFC to the primary mirror can be identified by their blue casings. The focal plane assembly (FPA, at the top of the structure) is supported by a fixed hexapod for alignment and a rotational stage that keeps the orientation on sky during a track.

Differences between the new tracker and the previous HET tracker include the provision of a center drive on the y-axis (rather than a side drive screw) and the addition of a constant-force drive (CFD) winch system as a safety measure on the y-axis. Both changes were necessitated by the significantly higher moving mass and analysis that showed unacceptable forces generated by impact of the tracker payload should there be a run-away in the y-axis, down-hill. The constant force drive uses an independent drive system with load-cell feedback to un-weight part of the load, but its primary purpose is to sense a runaway condition and apply a brake that is independent of the rest of the control system. This scheme provides safety for both equipment and personnel, and was settled upon following a detailed failure modes and effects analysis.

The hexapod actuators were manufactured by ADS International (Valmadrera, Italy) in collaboration with CEM and MDO[26]. A hydraulic test bed for the struts was built at CEM to test them in compression and tension over their operating range and to map residual errors in position versus encoder values. The actuator shaft rotations are encoded. The LT was used for this "mount-model" which exhibited only very small deviations from linear. Assembly into the hexapod configuration was first done in a vertical orientation. Following tests and initial characterization the assembled hexapod was mounted at 35 degrees in its test stand to mimic the posture on HET. In this configuration the control system was tested and positions confirmed with the LT to verify algorithms. The hexapod was subsequently mounted on the Y carriage following testing of the x- and y-axes with a dummy test mass on the carriage.

The tracker motion control system (TMCS) is based in the Matlab-Simulink environment in a dSPACE controller[29]. The Telescope Control System (TCS[30]) handles all the high-level functions and most of the coordinate transforms and mount models for the tracker. Limitations within the TMCS environment limit the ability to perform complex calculations on the 2.5 ms update rate, so TCS interprets all the higher-level functions for the TMCS and receives status updates 5 times per second through the API. Development of the TMCS at CEM lagged significantly and necessitated MDO personnel taking over responsibility for the system. While the tracker was dismantled and being installed we built a software model for the tracker to enable further development of the TMCS and the TCS in concert. This proved invaluable, since several architecture issues with the TMCS were not uncovered and fixed until this phase. The TCS-TMCS commands the tracker from the command line and the GUI level and executes moves and tracks and guides as needed for commissioning and early science operations.

4. WIDE FIELD CORRECTOR

The new corrector (Fig. 4) has improved image quality over a 22 arcminute diameter field of view and a 10 m pupil diameter. The periphery of the field is used for guiding and wavefront sensing to provide the necessary feedback to keep the telescope correctly aligned. The WFC is a four-mirror design with two concave 1 meter diameter mirrors, one concave 0.9 meter diameter mirror, and one convex 0.23 m diameter mirror. The corrector is designed for feeding optical fibers at f/3.65 to minimize focal ratio degradation, and so the chief ray from all field angles is normal to the focal surface. This is achieved with a concave spherical focal surface centered on the exit pupil. The primary mirror spherical aberration and the off-axis aberrations in the wide field are controllable due to the first two mirrors being near pupils, and the second two mirrors being well separated from pupils to control field aberrations. The imaging performance is 0.6 arcsec or better over the entire field of view, and vignetting is minimal. The WFC was manufactured by the University of Arizona College of Optical Sciences (OSC)[13-15].

Figuring and polishing of the three large mirrors was done at OSC on robotic swing-arm machines and tested with swing-arm profilometry using non-contact sensors. The degree of aspheric departure and the steepness of the surfaces of the large mirrors proved a challenge. Testing of the large mirrors used a combination of non-contact swing-arm profilometry, tied to laser tracker measures of the radius of curvature, and Interferometric confirmation of figures using phase etched computer generated holograms (CGHs) is proceeding. Testing was completed in March 2013. As part of the figure test, centering fixtures were aligned that were intended to be used in the final alignment of the WFC assembly. These center fixtures have CGH targets that provide a reference that locates the center and normal of each mirror surface. The smaller M4 was subcontracted to Precision Asphere, and utilized a transmission test with CGH.

Reflective coatings for the WFC are required to have high reflectance (95% or better from 350 nm 1800 nm), and are challenging, being based on silver and multiple dielectric layers. Experience with coating degradation on the old HET corrector led us to adopt a sealed design for the WFC with entrance and exit windows and careful sealing of the WFC housing. The WFC will be purged with nitrogen gas. The facility will have a large volume of nitrogen available from the cooling system for VIRUS, and this will be utilized to provide an over-pressurized oxidation-free environment for the mirror coatings to achieve the longest life possible. The large mirrors were coated by JDSU and M4 will be

recoated in August by Zecoat following failure of the initial coating by a different vendor. M4 sees a very wide range of incident angles, and requires a more complex coating than the others. MDO designed and constructed the complex fixturing needed to safely support the large mirrors during cleaning and coating at JDSU[31].

The structure of the WFC is a space frame, which is mounted kinematically into the PFIP and tracker (Fig. 4). FEA analysis focused on maintaining critical alignments between the mirrors as the corrector moves between the extreme angles of 25 to 45 degrees. In particular the separation of M4 and M5 has to be held to a few microns, and their very different masses make this a challenge. OSC designed tunable flexures for the M4 supports that allow the relative motion of these two mirrors to be tuned. MDO supplied test masses that mimic the mass and center of gravity[31] of the mirrors to allow testing of the structure and tuning of these flexures prior to completion of the mirrors. Tests with a laser tracker indicated all displacements were within specification and allowed tuning of the flexures to null out the relative motion of M4 and M5. The structure was thus qualified ahead of the completion of the mirrors.

The alignment scheme developed by UA OSC relied on the center references to locate the mirror surfaces using a combination of an interferometer and autocollimator to set centration and tilts and a LT to set separations. Then interferometric CGH tests of the M4/M5 pair the M2/3 pair and of the whole system were to be used to evaluate the alignment of the assembly. A conjugate test of the M4/5 pair with a custom wavefront sensor was developed by MDO staff to provide an independent confirmation that the system is meeting specification, particularly in off-axis performance[15].

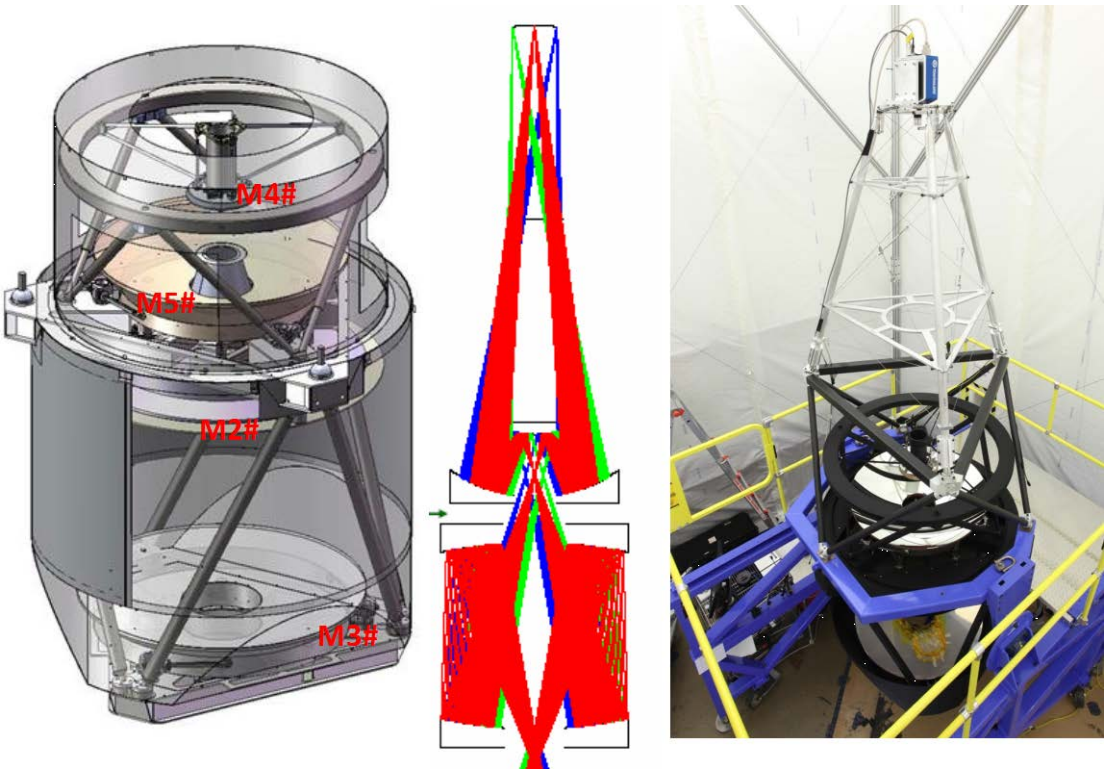

Figure 4. Layout of WFC mirrors and structure (left), and WFC structure undergoing tests with dummy mirrors to confirm performance and tune flexures for M4 supports (right).

The alignment process was initiated in September 2013 following integration of the mirrors into the WFC structure. It was discovered that the center references had drifted in tilt due to the choice of silicone to bond the references following alignment. Following diagnosis of this problem, an alternative alignment scheme utilizing the M2/3 and M4/5 subsystem interferometric CGH pair tests was developed to align in tilt. The center references were sufficient for centration and separation. In February 2014 this scheme was started with the M4/5 pair. Inconsistency in the wavefront measured for this pair indicated an error on the figure of one of the mirrors, which was eventually traced to M5 having a significantly different figure than established in the original tests, due to errors in analysis[14,15]. Subsequent review

revealed a significant error in M3 also. Following an extensive period of review, and execution and analysis of the M4/5 CGH pair test, the M2/3 CGH pair test and the UT M4/5 conjugate test, we achieved an understanding of the figures of each mirror within the required error bounds to meet specification.

Figure 5: Images of completed HET WFC being transported and installed. (a) WFC in its handling cart next to transportation box; (b) WFC arriving at HET after overnight transportation; (c) WFC mid-air being hoisted into position in the HET tracker.

The spacing of mirrors in the prescription of the WFC was re-optimized by MDO in conjunction with an aspheric corrector plate and a separate configuration for the atmospheric dispersion corrector (ADC). The resulting prescription met the original image quality requirements. OSC proceeded to align the corrector, and MDO procured the aspheric corrector plate. Since the corrector should now be regarded as being a 5-element design, including the corrector plate, the system test included the corrector plate. The reflective CGH in the system test essentially mimics the wavefront from the primary mirror, so the system test provided confirmation of the final delivered wavefront, expected on-sky, on axis.

The final test procedure and results are discussed in Ref. 15). The loss of center reference information led to uncertainties in the final state of the WFC after interferometric alignment, since the null-tests had to be used for alignment, not just verification. As a result, the on-axis tests could hide degeneracies, particularly in the alignment of the M4-M5 pair, which controls the off-axis aberrations and are crucial for the ultimate wide-field performance of the HET. Motivated by the need to gain more information prior to shipping the WFC form the UA facility, UT added a conjugate test utilizing a Shack-Hartmann wavefront sensor that allowed for some off-axis information to be gathered[15]. The results were analyzed and reviewed, with the conclusion that there was some residual misalignment uncovered by the conjugate test, manifesting in a tilt of the focal surface that could place the WFC performance outside acceptable bounds. The issue was that, in order to keep the position angle fixed on sky during a track, the physical focal surface must rotate relative to the fixed WFC, so a tilted optical surface could not be aligned simply by tilting the focal plane assembly to match. However, the majority of realizations of the state of the WFC allowed by the conjugate test data resulted in tilts well within specification with only two that placed it outside specification. Following external review of the results, it was agreed that the WFC likely would meet specifications and the only way to gain further information was to integrate it with the HET primary mirror and perform on-sky testing to verify the system.

The WFC was transported (very carefully and at night) to HET on May 28, 2015[15,32]. Following a repeat of the interferometric system test inside the HET facility, to verify that there had been no movement of mirrors during transportation, we installed the WFC on HET on July 2, 2015, followed by the PFIP, which was aligned to the WFC

optical axis using a laser tracker and an alignment telescope, referenced to a target at the center of the Input Head Mount Plate (IHMP, see below) that defines the physical focal surface. Alignment of the WFC to M1 was achieved by direct measurement with an alignment telescope hung under the WFC and aligned to the center reference on M4 in the WFC that defines its optical axis. The alignment telescope was then reversed in its mount to point at the center segment of M1 and aligned (in X,Y, and tip/tilt) with cross hairs strung across that segment, by introducing offsets in the tracker position. These offsets were small (on the order of 20 mm, indicating the accuracy of the tracker setup) and defined the center of the track from an optical perspective. Reversing the alignment telescope again to look out of the dome at the CCAS tower, we verified that the optical axis of the telescope was aligned very closely to the entrance aperture of the CCAS alignment instrument that defines the center of curvature of the primary mirror. This confirmed that the axis is aligned with the primary mirror center of curvature as defined by the source in the Mirror Alignment Recovery System (MARS[37]) in the center of curvature tower, which is used to stack the mirror segments to a common center of curvature at the start of each night. We had completed a dry-run of this alignment procedure using a dummy corrector, while we waited for the WFC to be completed, so this procedure was completed in a few days and we achieved first light on July 29th 2015, immediately achieving good pointing within an arcminute, and excellent image quality on the acquisition camera (1.3 arcsec FWHM, consistent with the expected median image quality of the system).

5. PRIME FOCUS INSTRUMENT PACKAGE

The PFIP[18,19] rides on the tracker and consists of several subassemblies. The Wide Field Corrector (WFC) mounts on a strongback on a three ball-in-vee kinematic mount. The strongback mounts to the tracker hexapod and the structure of PFIP is built up around the corrector. The focal plane assembly (FPA), shown in Fig. 6, contains all the hardware at the focus of the telescope including the acquisition and guiding (AG) assembly, fiber instrument feeds, shutter, and electronics hardware. The Lower Instrument Package (LIP) is mounted to the input end of the wide field corrector and is a platform for the entrance window changer, tip-tilt camera, and facility calibration unit (FCU) output head. A set of temperature controlled, insulated enclosures house electronics hardware and the FCU input sources, optics, and selection mechanisms. The pupil plane assembly (PPA) is located in between the wide field corrector and the focal plane assembly. It contains a stationary and moving set of baffles at the exit pupil of the telescope and a platform for selectable exit windows (aspheric corrector plates) and the atmospheric dispersion compensator (ADC) for the wide field corrector. The deployment of the PPA has been split into two phases. Initially, the support structure with fixed exit pupil baffle and the corrector plate have been deployed. Since the design of the PPA has to be updated to accommodate the tighter positioning requirements of the corrector plates (one each for optical and NIR bandpasses) the full system will be built and deployed after the HET is commissioned and resources are available for this additional effort.

The heart of the metrology system for the WFU is the AG assembly (Fig 6 & 7), which mounts the guide probe assembly, the acquisition camera, a wavefront sensor and a pupil viewer. The light is directed to these by deployable pickoff mirrors with pneumatic actuators. The guide probe assembly is used for star guiding of the telescope and wavefront sensing feedback to the telescope focus. There are four probes; two imaging probes and two wave-front sensing probes. Each probe consists of a probe optical head, containing the necessary optics coupled to a coherent fiber bundle purchased from Schott. Images incident to the fiber bundle input are captured by a remote camera system (FLI Proline) at the bundle output, fed by reimaging optics and including a filter wheel for each of the guide probes. Each probe optical head is mounted to a carriage with an arm for moving the probe radially in the field with a range of 9-11 arcminutes from the center of the telescope's field. The four carriages each move through 180^{O} sectors on large bearings to access stars (Fig. 7). The positioning accuracy requirement of the guide probes is 20 microns on the spherical focal surface. To achieve this, both mechanical position actuation and encoding required a high level of precision. The acquisition camera has 3 arcminute field of view and can be used simultaneously with the GPs and WFS in the guide probe assembly.

The prime focus shutter, which shutters VIRUS and LRS2 is a rotary-type shutter initially inspired by the VLT FORS shutter design. The carbon fiber reinforced plastic (CFRP) shutter "blade" is a rotating disc with an aperture cut out of one section. Exposure occurs when the disc rotates so that the aperture aligns with the clear aperture of the focal surface. The shutter blade is fastened to a hardened steel ring. The inner diameter of the ring has a vee profile, which rides on 6 ball-bearing guide wheels mounted to the shutter chassis. The outer diameter of the ring has a toothed profile which meshes with a Kevlar reinforced toothed drive belt. The belt is driven by a toothed pulley driven by a DC servo motor. An absolute rotary encoder is mounted at the center of the shutter blade. A flexural mount on the encoder body ensures concentricity between encoder axis and shutter axis. The timing and position control of the shutter is achieved using position, velocity, and time (PVT) trajectory interpolation. Minimum required exposure is 1 second, which is

achieved by ramping up to a constant velocity. Longer exposures typically have an open command and a close command with a pause between for the exposure time. Pre-deployment tests verified 5 millisecond accuracy for the timing of the shutter over thousands of actuations. Lifetime testing has already logged the equivalent of several years of operations.

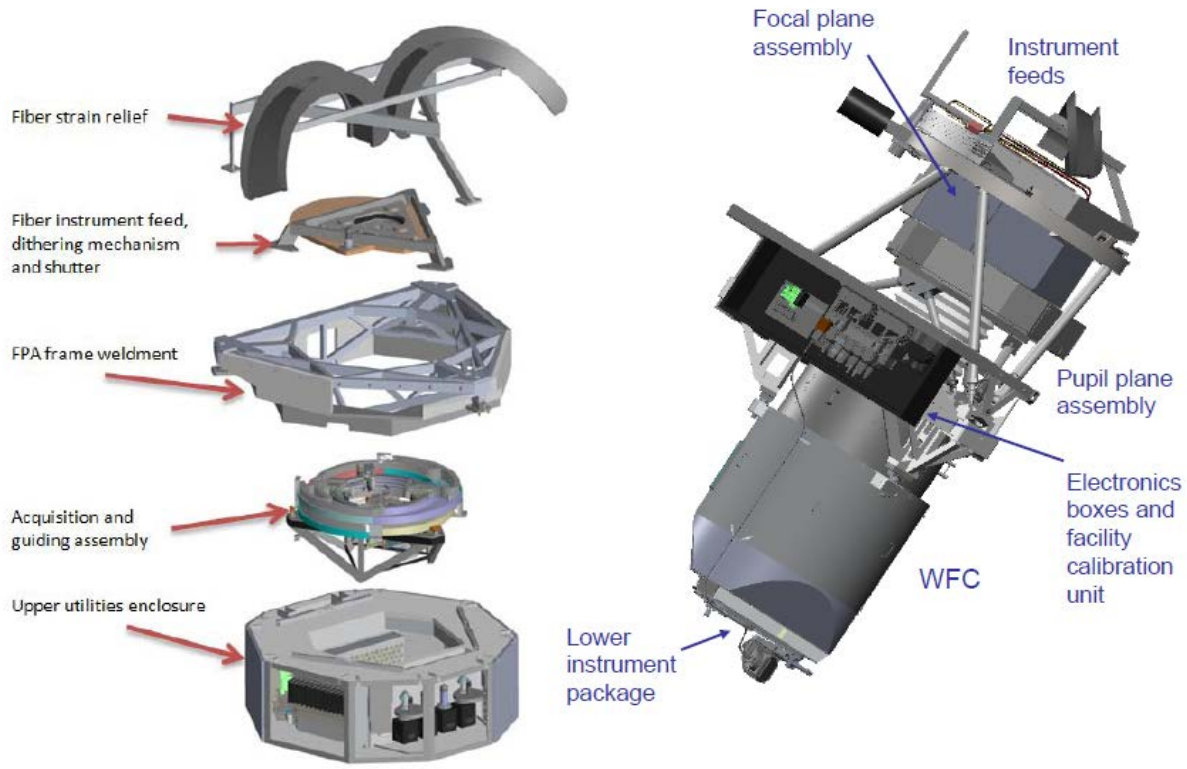

Figure 6. Renderings of the PFIP. On the right the full assembly is shown with major sub-assemblies indicated. On the left is an exploded view of the FPA showing its major components. The FPA contains most of the complexity of the instrument, including the acquisition and guiding (AG) assembly with guide probes and wavefront sensors.

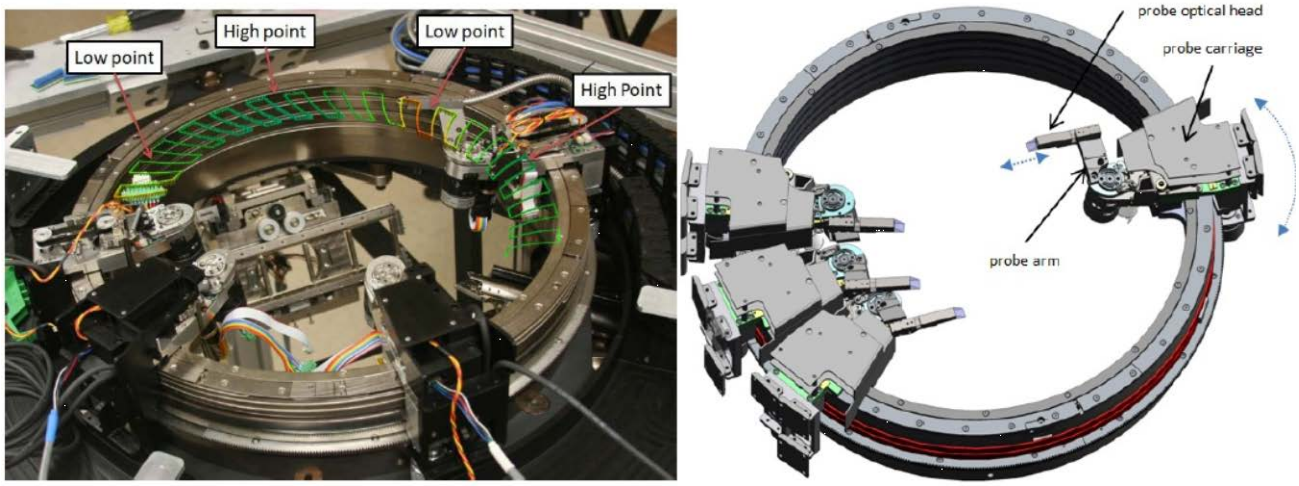

Figure 7. Guide probe assembly. Left shows the assembly undergoing performance tests with the LT. Peak to peak error is 30 microns, well within specification for focus. The layout and ability for the probes to nest very closely while avoiding any collision is shown on the right.

The dithering mechanism (Fig. 8) is a three position actuator that mounts the input head mount plate (IHMP) for the fiber feeds offsets fibers so that a set of three exposures will fill the interstitial space between fibers in a single VIRUS IFU[33-35]. The device is actuated by six Festo "fluidic muscle" pneumatic actuators; two are active in each of three positions. These actuators were selected for their high initial force and small diameter. They are particularly well suited for short-throw applications. A special pin flexure of titanium was designed to control the motion of the dithering mechanism. The design required a ~150 micron movement in a plane normal to the optical axis but only allowed for ~5 micron motion parallel to the optical axis despite the varying loads expected from the fiber feeds. Repeatability of motion has been demonstrated to be 5 microns rms, unloaded.

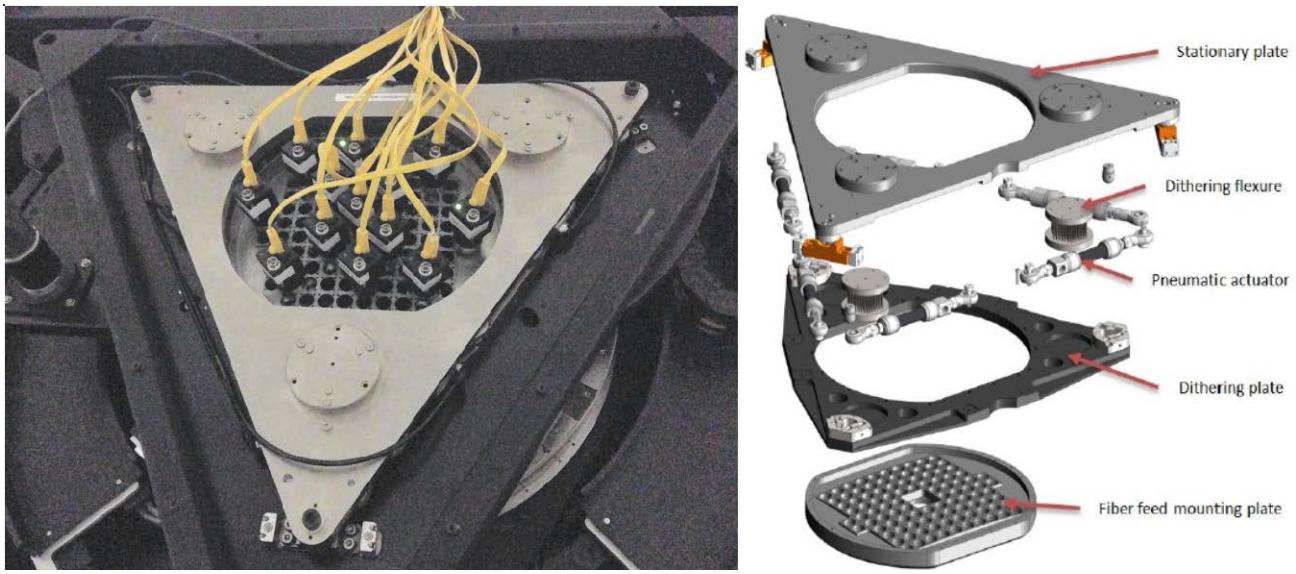

Figure 8. Dither mechanism that moves the VIRUS IFU heads between three precisely defined and repeatable positions. The exploded view on the right shows the components. The titanium flexures ensure that the assembly will carry the loads it will see during operation and still allow the small motions required. Left shows the assembled mechanism mounted on HET. This view shows small deployable wavefront sensors (dWFS) installed for the evaluation of the WFC image quality over the full 22 arcminute field of the upgraded HET

The LIP mounts to the WFC directly, and houses the entrance window selector and the facility calibration unit (FCU) input head. The FCU illuminates the pupil and focal surface of HET with a pattern that mimics that obtained on sky[36].

The PFIP has many precision mechanisms and is required to meet specifications over a temperature range of -5 to 25 Celsius, and operate down to -10 Celsius. In order to test the PFIP environmental specifications, we undertook an extensive program of cold-testing, including all mechanisms and cameras being constantly moved over a period of three days and nights. We utilized a rented refrigerated truck for these tests and took the PFIP and FCU through several temperature cycles over the test period[19].

PFIP was deployed on HET in July 2015. The alignment to the WFC is described above. PFIP is a very complicated instrument in its own right, and has been commissioned in phases from July 2015 to May 2016. Most commissioning effort has been in establishing frames of reference for the various cameras within the higher-level control software. The GPA has been commissioned and integrated into the system to the point where setup on a field results in all probes being centered on their target stars. We have also commissioned guider controlled offsetting between the two IFUs of the LRS2 instrument so that beam-switching between them can be achieved. The guide probes move in sympathy with the offset so that

6. METROLOGY SYSTEMS

HET requires constant monitoring and updating of the position of its components in order to deliver good images. The WFC must be positioned to 10 μm precision in focus and X, Y, and 4.0 arcsec in tip/tilt with respect to the optical axis of the primary mirror. This axis changes constantly as the telescope tracks, following the sidereal motions of the stars.

Tilts of the WFC cause comatic images. In addition, the global radius of curvature (GROC) of the primary mirror can change with temperature (as it is essentially a glass veneer on a steel truss), and needs to be monitored. The segment alignment maintenance system (SAMS) maintains the positions of the 91 mirrors with respect to each other, but is less sensitive to the global radius of curvature of the surface. The feedback to maintain these alignments requires excellent metrology, which is provided by the following subsystems:

- Guide probes to monitor the position on the sky, and plate scale of the optical system, and monitor the image quality and atmospheric transparency
- Wavefront sensors (WFS) to monitor the focus and tilt of the WFC
- Distance measuring interferometer (DMI) to maintain the physical distance between the WFC and primary mirror
- Tip-tilt sensor (TTS) to monitor the tip/tilt of the WFC with respect to the optical axis of the primary mirror

The upgrade adds wavefront sensing[20-22] to HET in order to close the control loop on all axes of the system, in conjunction with the DMI adapted from the current tracker metrology system and a new TTS[18]. There is redundancy built into the new metrology system in order to obtain the highest reliability. Two guide probes distributed around the periphery of the field of view provide feedback on position, rotation, and plate scale, as well as providing a record of image quality and transparency as a function of wavelength. The alignment of the corrector is monitored by the wavefront sensors as well as by the DMI and TTS. The radius of curvature of the primary mirror is monitored by the combination of focus position from the WFS with the physical measurement from the DMI and checked by the plate scale measured from the positions of guide stars on the guide probes. The SAMS edge-sensors provide a less sensitive but redundant feedback on radius of curvature as well.

The two guide probes use small pick-off mirrors and coherent imaging fiber bundles to select guide stars from the outer annulus of the field of view. They are located ahead of the focal surface, before the shutter. Each ranges around the focal surface on precision encoded stages, accessing a 180 degree sector. They are designed to have a small size to reduce shadowing of the focal surface, and each has a field of view of 22.6 arcsec on a side. During setup on a new target, they will be driven to pre-defined positions, and the initial pointing will be made by centering the guide stars in the probes. This system is a significant upgrade from the former pellicle-based guiders on HET.

Two Shack-Hartmann (S-H) wavefront sensors also range in the outer field. Their function is to provide feedback on the low-order errors in the wavefront (focus, coma, spherical, and astigmatism)[20-22]. These errors are caused by misalignment of the corrector with the primary mirror focal surface and by global radius of curvature and astigmatism errors in the primary mirror shape. Updates will be generated approximately once per minute. In addition to the WFS probes there is an analysis wavefront sensor, selectable within the FPA by deploying a pickoff mirror, that will allow more detailed feedback analysis of the image quality, simultaneous with the operation of the WFS probes, independent of seeing. Simulations show that a S-H system with 7x7 sub-apertures across the pupil can meet the requirements using 18th magnitude stars and this is being borne out as we commission the system. The design of the wavefront sensors is straightforward, but their application to the HET, with the varying illumination of the telescope pupil during a track, requires development of a robust software system for analysis of the sensor data to produce reliable wavefront information.

7. SOFTWARE

The new integrated software control system for the HET WFU is described in Ref. 30. It uses a component architecture providing a high degree of monitoring, automation, scriptability and scalability. It consists of a network of control systems, each of which models a sub-set of closely coupled hardware. The control systems (CS) communicate with each other using simple but flexible messaging scheme encoding commands to subsystems and events informing of state changes. Each system is responsible for specific functions based on type or proximity to hardware, and is designed to be run autonomously. For engineering purposes, each subsystem can also be scripted independently of others. The primary systems for the WFU and VIRUS are the Telescope CS (TCS), the Prime Focus Instrument Package CS (PFIP-CS), the Payload Alignment CS (PAS), the VIRUS Data Acquisition CS (VDAS), and the Tracker motion CS (TMCS), along with a centralized logging system. In addition to these control systems, GUI interfaces for the telescope operator and resident astronomer have been developed. The TCS is responsible for coordinating the operation of all other CS and knowledge of the high-level astronomy-related state is restricted to TCS. PFIP-CS controls the hardware on PFIP, while the PAS is responsible for gathering metrology from various alignment systems, including the guiders, WFS, TTS, and the DMI needed to close all tracker-motion related loops. The logger is failsafe, logging into local databases if the central log-server is down. These local databases are synchronized automatically with the central log server when it is

available. In addition to log messages, logging can be configured to log any subset of events generated by the system, to obtain very detailed execution traces. This is done without interfering with the operation of the CS generating no additional overhead or changes in timing. The primary operating system is Red Hat Enterprise Linux 6.x, 64-bit. The software was developed with an agile process using the standard GNU toolchain, and widely available libraries. The TCS has been controlling the telescope since delivery of the tracker and is now a mature system. The software for VDAS is controlling 16 deployed VIRUS units and LRS2.

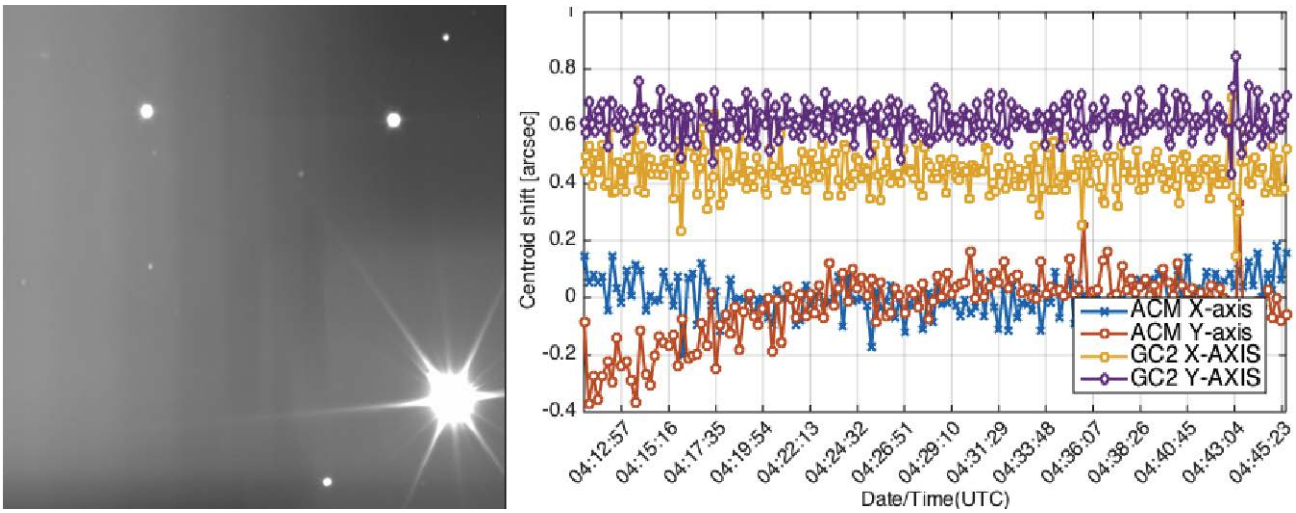

Figure 9: Left - first light image with upgraded HET obtained in the g band on July 29, 2015. The full 3 arcminute field of view of the acquisition camera (ACAM), located at the center of the HET field of view, is shown. Image quality was measured at 1.30 arcseconds FWHM over field. Right – example of HET guiding with one guideprobe and ACAM being monitored for a full track. Note the small dispersion in GP positions of 0.15 arcsec. rms, and the position shift seen on the ACAM at the extremities of the track. This shift is a feature of the changing pupil illumination of HET during a track and is expected. See text for details.

8. FULL-FIELD IMAGE QUALITY & MOUNT MODEL VERIFICATION

The first light image obtained with the ACAM is shown in Fig. 9. Achieving good on-axis image quality at first light did not vindicate the alignment of the WFC, however, due to the residual uncertainties discussed above, so over the Fall of 2015 we undertook on-sky tests with miniature wavefront sensors deployed over the field of view (mounted in the VIRUS IFU seats in the input head mount plate (IHMP), see below) as a final confirmation of the performance of the WFC. By this point we were able to track both sidereal objects and geostationary satellites (GS) with high reliability. Testing of the WFC alignment required us to set up a GS on each of the dWFS in turn, measuring the wavefront as a function of field position. Details of these tests and analysis are provided in Ref. 15. We were relieved to detect only a small tilt of the optical focal surface relative to the IHMP, within specifications, and could eliminate the possible scenarios that would have failed our requirements.

Subsequent testing using the ACAM and GPs has shown excellent IQ over the whole field, dominated by site seeing and the primary mirror, so the WFC has met all its requirements, and indeed contributes negligibly to the delivered IQ under typical conditions. Subsequent testing with the first deployed IFUs of VIRUS has confirmed excellent image quality across the field through observations of dense globular cluster star fields[10].

The original HET system utilized a heuristic mount model based on on-sky measurements, which convolved the many physical effects that contribute to the pointing and tracking accuracy of the integrated system. Adjustments to improve pointing would often result in poorer tracking accuracy, and vice-versa. For the WFU, we set out to base the mount model on direct physical measurement of subsystems that could be combined to create a deterministic correction to the tracker position with well-understood physical underpinnings. Our primary tool in this was laser tracker and SMR retro-reflectors, which we utilized to understand the deflections of the tracker subsystem, using a dummy WFC to mimic the load. These measurements created a transform with low-order terms that accounted for the deflections of the tracker relative to the ideal tracking sphere. These measurements were further refined using the TTCAM and DMI to provide direct measurements of the payload relative to the surface of M1, and thereby tie the tracker frame to the optical frame provided by the primary mirror, aligned by the CCAS instrument.

The telescope structure sits on 4 feet on a very flat concrete pier. Deflections of the telescope structure during the track, due to the unbalanced loading as the payload moves in X,Y, were also measured against the telescope pier and incorporated as a further layer of mount model terms that transform the tracker frame to the projection on sky. As the telescope is moved in azimuth to access different declinations there is also a term in the pointing mount model that accounts for the non-flatness of the pier. This approach to the mount model has proven very successful with pointing residuals already meeting requirements and goals in the central half of the tracker range. Just as important, drift rates are very low and correlate closely with pointing residuals, which indicates that improvements in one will be reflected in the other. This has been our experience to date, and we expect ongoing work to yield pointing and tracking within specification over the whole HET tracker range.

9. VIRUS INFRASTRUCTURE

The VIRUS spectrograph units take up a large volume and require a distributed liquid nitrogen (LN) cooling system[11]. The infrastructure to support VIRUS is a significant undertaking and is being integrated with the deployment of the WFU. Since the wavelength coverage of VIRUS extends down to 350 nm, the average fiber length had to be minimized commensurate with keeping the mass of the instrument off the telescope structure and providing sufficient access to the primary mirror and tracker with the HET man-lifts and crane. Following extensive optimization and evaluation by HET staff, we settled on a configuration with VIRUS units housed in two large enclosures flanking the telescope structure (Fig. 10) and riding on a separate air-bearing system during rotation of the telescope in azimuth (Fig. 1).

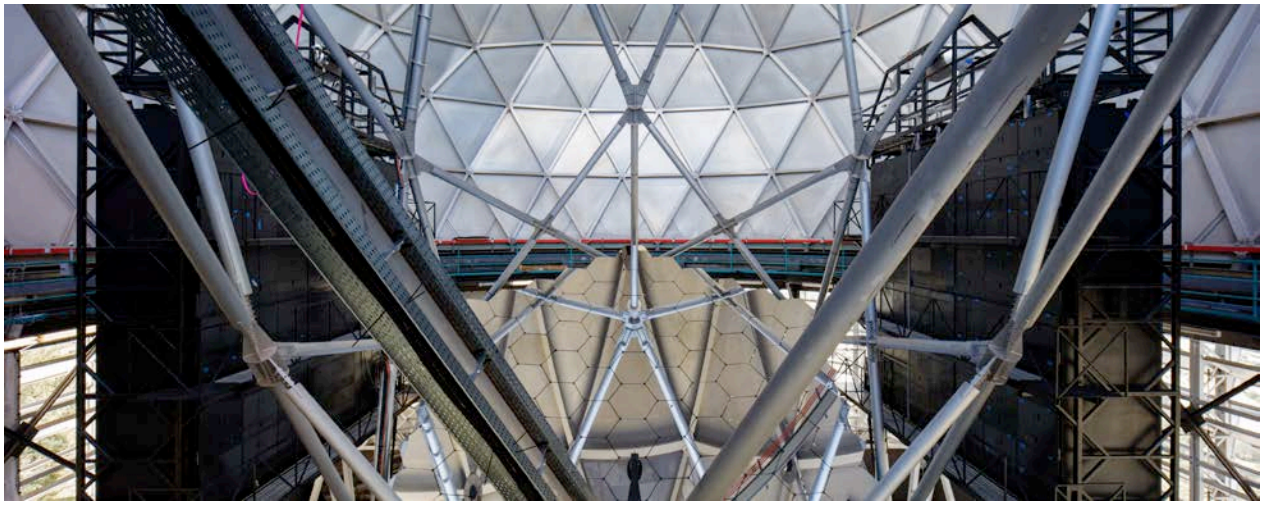

Figure 10: View of the HET from the front showing the primary mirror and the large VIRUS enclosures either side of the telescope structure. They sit on the VIRUS support structure (VSS), which moves on air bearings to follow the azimuth setting of the telescope. The phase separator tanks of the VIRUS Cryogenic System (VCS) can be seen mounted to the top of each enclosure.

VIRUS units and the new LRS2 low-resolution spectrograph are housed in the large enclosures mounted on each side of the telescope. They are supported by the VIRUS support structure (VSS[24]) framework designed to carry the weight of the enclosures and spectrographs without connecting to the main structure of the telescope in order to ensure no coupling of wind-shake-induced motion into the tracking of the telescope[6]. For changes in azimuth, the VSS rides on its own set of air bearings and is dragged by the main structure drives through loose linkages. When the structure is placed down, there is no significant coupling between the structures except through the concrete ring-wall pier at the base.

The two large VIRUS enclosures are mounted to the VSS and are essentially sealed clean-rooms with a heat removal system to avoid degradation of the seeing by the heat generated by the detector controllers and electronics from escaping to the dome by convection or air leaks. They are based on large steel space-frames manufactured by SMK Manufacturing with skins and removable hatches to provide access to both sides of the spectrograph for camera

maintenance and IFU access, respectively. The weldments were procured by MDO and were outfitted with hatches, seals, cables and the heat removal system by TAMU[37]. The lightweight foam-core hatches were produced in quantity and have shown excellent performance for air leakage rate.

The heat removal system is separate for each enclosure and uses ambient temperature facility glycol as the primary coolant fluid with a 600 W "Thermocube" thermoelectric cooler providing the ability to tune the temperature of the circulating air to keep the overall environment close to ambient temperature. It is needed to keep the VIRUS detector controllers from overheating and to remove the heat they generate so it does not enter the dome and degrade the seeing environment. Air is drawn through the controllers by the system with dampers set to even out the air flow among the controllers, and cold HEPA-filtered air is returned at the top of each sealed enclosure[37].

The distributed and large-scale layout of the VIRUS array presents a significant challenge for the cryogenic design[10,38,39]. Allowing 5 W heat load for each detector, with all losses accounted for and a 50% margin, the cooling source is required to deliver 3,600W of cooling power. We engaged George Mulholand of Applied Cryogenics Technology to evaluate the options and provide an initial design. Following a trade-off between cryocoolers, small pulse-tubes and liquid nitrogen based systems, it is clear that from a reliability and cost point of view liquid nitrogen is the best choice[35]. The problem of distributing the coolant to the distributed suite of spectrographs is overcome with a gravity siphon system fed by a large external LN tank. A trade-off between in-situ generation of the LN in an on-site liquefaction plant, and delivery by tanker has been made, with the result that the delivery option is both cheaper and more reliable.

An important aspect of the cryogenic design is the requirement to be able to remove a camera cryostat from the system for service, without impacting the other units. This is particularly difficult in a liquid distribution system. A design has been developed that combines a standard flexible stainless steel vacuum jacketed line (SuperFlex) to a cryogenic bayonet incorporating copper thermal connector contacts into each side of the bayonet. When the bayonet halves are brought together they close the thermal contact. The resulting system is completely closed, i.e., it is externally dry with no liquid nitrogen exposure. The camera end of the connector is connected by a copper cold finger to the detector. This design has another desirable feature: in normal operation the SuperFlex tube slopes downwards and the bayonet is oriented vertically. Liquid evaporation will flow monotonically up in order to avoid a vapor lock. If the bayonet is unscrewed and raised upwards, a vapor lock will occur and the bayonet will be cut off from the cooling capacity of the liquid nitrogen. This effectively acts as a "gravity switch", which passively turns off cooling to that camera position.

We have made extensive tests on prototypes, applying heat loads to the bayonet, which have performed very well[39]. The temperature rise across the connection is $\Delta T \sim 1.8$ K/Watt of load at 80 K. Modeling of the full thermal path has been undertaken, under the requirement of having the CCD temperature at -140 C, with no heater power. The performance of the bayonet is significantly better than the requirement, and represents less than 20 K temperature rise across the connection for the expected load. We run the CCDs at about -100 C, controlled via heating resistors and a control loop based on an RTD sensor.

The contract for the fabrication of the VCS was awarded to Midwest Cryogenics. In the process of working with Midwest Cryogenics we discovered issues associated with the manufacturability and maintainability of our initial design[38,39] for the VCS components that reside in/on the VIRUS spectrograph enclosures. After working closely with Midwest Cryogenics a much-improved design emerged. Before proceeding with fabrication, a full-scale prototype of one of the vertical distribution pipes was fabricated and functionally tested at Midwest Cryogenics. The test verified that the pipe sizes would not compromise the two-phase flow thereby reducing the system's ability to remove heat from the camera cryostats.

The 11,000 gallon vacuum jacketed tank was installed by Praxair in October 2014. The enclosures were delivered to HET and the VCS installed in Nov 2014 and Feb 2015. The system was first turned on in Feb 2015. Currently, spectrographs in only one of the enclosures are being cooled. In full operation we will have in excess of 4 weeks capacity and a 6,000 gallon delivery of LN will be required every two to three weeks. Praxair is making regular deliveries triggered by metrology on the main tank that indicates LN level.

An essential part of VCS is its safety system. This system continuously monitors critical variables (e.g. dome atmosphere oxygen levels, LN pressure, LN flow rates, and LN storage tank levels). When predefined set points are exceeded the system automatically activates strategically located audio and visual alarms, and if required closes the main LN supply line valve. The heart of the safety system is a Sensaphone SCADA 3000. It can handle up to 144

digital/analog I/O channels and can automatically place telephone calls (with prerecorded messages) to operations personnel. Safety system power is derived from a single UPS that is dedicated 100% to the safety system, and is backed up by the facility generator. Each afternoon the system undertakes an auto-test of the alert system, and sends test telephone alerts to the recipient list. This ensures that the system cannot go off-line for an extended period without being noticed.

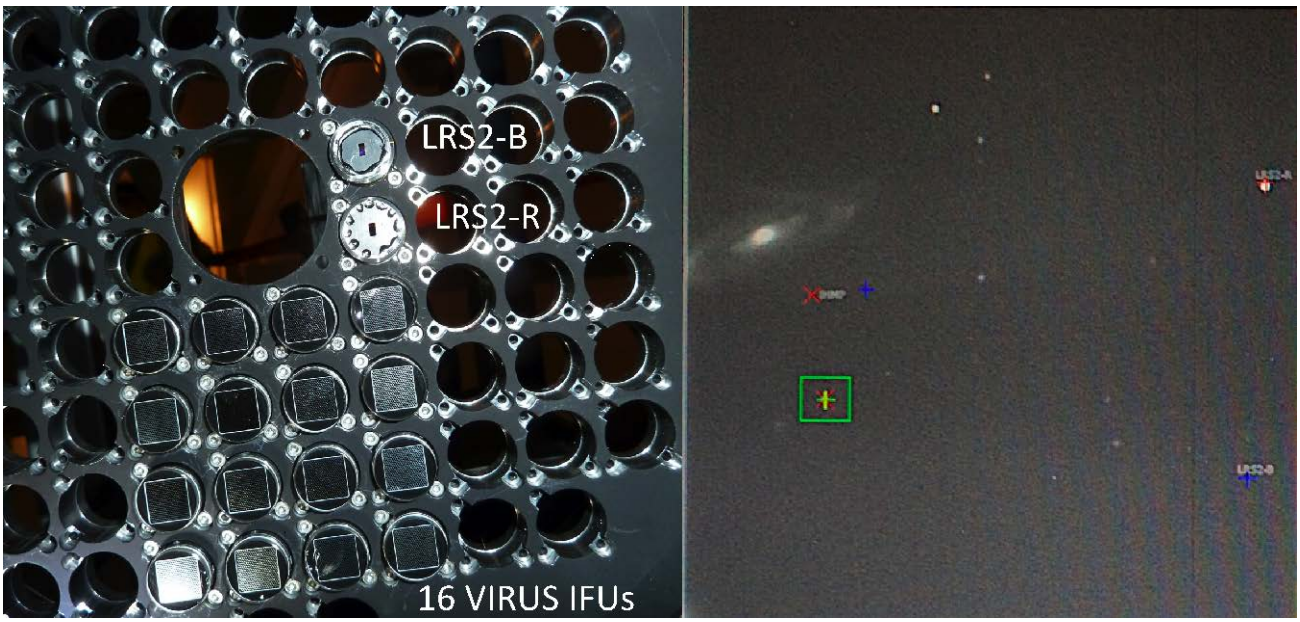

Figure 11: Left – photon's-eye view of the first deployment of IFUs for LRS2 and VIRUS mounted in the IHMP; LRS2 has two small full-fill IFUs mounted close to the central circular mounting boss for the high resolution spectrographs. LRS2-B is at the top and LRS2-R below it; they are 100 arcsec. apart on the sky. 16 VIRUS IFUs can also be seen arrayed in a 4x4 grid. Right – example ACAM image of setup of a supernova on the LRS2-R IFU. The field of view is 3 arcminutes and the host galaxy can be seen on the left. The fiducials for the optical axis (red X), LRS2-B (blue +), LRS2-R (red +), and a setup star used to execute a blind setup (yellow + and green guide box) are shown.

10. CURRENT PERFORMANCE AND REMAINING WORK

In the 11 months since first light we have verified the optical performance of the upgraded HET, refined the mount models, installed and commissioned the new Low Resolution Spectrograph (LRS2[23]), and installed the first 16 VIRUS units[10] (Fig. 11). We will enter early science operations of the HET with LRS2 in queue mode on July 1, 2016. The remaining work to complete the WFU system centers on the commissioning of the WFS system. The two OWFS are part of the GPA and are positioned on stars to provide real-time feedback on focus and corrector tilt during a track, via low-order wavefront sensing. In conjunction with the DMI, which measures the physical separation of WFC from M1, the focus of the system can be maintained and the GROC of M1 monitored. As the ambient temperature changes during the night the telescope structure and M1 truss change size with a coefficient of expansion of steel, and we will adjust the GROC of M1 using SAMS between tracks. We have obtained measurements demonstrating these feedback loops and we expect to complete commissioning of this remaining metrology system over the summer.

Figure 9 shows an example of guiding stability during a full track. The small guide residuals are evident (see Table 1). The right hand panel of Fig. 9 shows the detection of a differential drift between the GP (located at the edge of the 22 arcminute field) and the ACAM, located at the center. The drift occurs most at the extremes of the track and it is an expected feature of the HET design due to the changing pupil illumination throughout the track. This drift is expected, but was never detected with the old HET. Here is us clearly resolved and will be corrected via software offsets based on models of the centroid shift with pupil illumination and by employing two GPs to average out the effect.

Table 1: High-level performance requirements for HET upgrade, compared to performance of the "old" HET and current performance of the HET WFU (characteristics in *italics* are based on limited data obtained so far in commissioning)

Performance area	Requirement	"old" HET	Upgraded HET	Comment
Pupil diameter	10 m class	9.2 m	10.0 m	At center of track
Field of view	22 arcmin diameter	4 arcmin	22 arcmin	70 times larger area at same level of field vignetting
Median on-axis image quality EE(50%)	1.25 arcsec EE(50%)	1.7 arcsec	*1.3 arcsec*	In median 1.0 arcsec site seeing
Open-loop pointing (rms)	25 arcsec (goal 9 arcsec)	30 arcsec	5-15 arcsec	Achieving 5 arcsec within central half of track range
Setup time (end of exposure to start of next)	< 5 minutes 90% of the time	7-20 mins	4-7 minutes	Upgrade can set up blind on invisible targets in same time
Setup accuracy	0.25 arcsec rms (0.1 arcsec goal)	0.5 arcsec	*0.15 arcsec*	Ability to center target on fiber, slit, or IFU; measured on LRS and LRS2
Metrology System	full sensing of all degrees of freedom	only guiding	*All degrees*	Current system has guiding and physical feedback on WFC alignment; wavefront sensing to be commissioned in July 2016
Guiding residuals	0.25 arcsec rms	0.5 arcsec	0.15 arcsec	Upgrade has 2 guider probes and 2 wavefront sensors

In parallel with the WFU installation, the primary mirror segments are being recoated with a dense Aluminum reflective coating in a new coating facility on site. By the time of resumption of full science operations in 2017, all segments will have been cycled through the facility. Recoating and cleaning with dry ice snow will be an ongoing effort to maintain the primary mirror reflectivity in the best possible state. Reflectivity will be monitored with a 3-color CCD camera pupil viewer in the FPA.

11. SUMMARY

HET was taken off line at the end of August 2013. The removal of the old spherical aberration corrector, PFIP, and tracker followed by the installation of the new tracker was complete in May 2014. A year later the WFC was delivered from UA OSC, and first light was achieved in July 2015. Testing of the system and refinement of the software and mount-models demonstrated that the WFU has achieved its goals. Instrument installation and commissioning started in November 2015 and the new HET enters early science operations with the new Low Resolution Spectrograph (LRS2) on July 1, 2016. During the remainder of 2016 the upgrade high-resolution spectrograph (HRS2[40]) is due to be installed, and more VIRUS units will be deployed. An infrared high resolution spectrograph called the Habitable-zone Planet Finder (HPF[41]) will follow. Full science operations will commence in early 2017.

ACKNOWLEDGEMENTS

HETDEX is run by the University of Texas at Austin McDonald Observatory and Department of Astronomy with participation from the Ludwig-Maximilians-Universität München, Max-Planck-Institut für Extraterrestriche-Physik (MPE), Leibniz-Institut für Astrophysik Potsdam (AIP), Texas A&M University (TAMU), Pennsylvania State University, Institut für Astrophysik Göttingen, University of Oxford and Max-Planck-Institut für Astrophysik (MPA). In addition to Institutional support, HETDEX is funded by the National Science Foundation (grant AST-0926815), the State of Texas, the US Air Force (AFRL FA9451-04-2-0355), by the Texas Norman Hackerman Advanced Research Program under grants 003658-0005-2006 and 003658-0295-2007, and by generous support from private individuals and foundations.

We thank the following reviewers for their valuable input at various stages in the project:

- Science Requirements Review 6-26-07, Roland Bacon, Gary Bernstein, Gerry Gilmore, Rocky Kolb, Steve Rawlings
- Preliminary Design Review 4-10-08, Bruce Bigelow, Gary Chanan, Richard Kurz, Adrian Russell, Ray Sharples
- PFIP Integration and Alignment Review 7-26-11, Larry Ramsey, Bruce Bigelow, Steve Smee, Mike Smith
- Tracker Factory Acceptance Test Plan Review 3-8-11, Povilas Palunas, Jeffrey Kingsley, Dave Chaney
- Wide Field Upgrade Readiness Review, 7-16-13, Daniel Fabricant, Fred Hearty

- Wide Field Corrector Pre-shipment Review 4-22-15, Daniel Fabricant, Fred Hearty
- VIRUS Detector System Review, 2-1-16, Roger Smith, Ian McLean, Phillip MacQueen

We thank the staffs of McDonald Observatory, the Hobby-Eberly Telescope, and the Center for Electromechanics, University of Texas at Austin, the University of Arizona College of Optical Sciences, and Department of Physics and Astronomy, TAMU, for their contributions to the HET Wide Field Upgrade. Our particular thanks go to Darragh O'Donoghue and Buddy Martin who acted as external reviewers during diagnosis of the figure error issues on the WFC. This paper is dedicated to the memory of Darragh O'Donoghue.

REFERENCES

[1] Booth, J.A., Wolf, M.J., Fowler, J.R., Adams, M.T., Good, J.M., Kelton, P.W. Barker, E.S., Palunas, P., Bash, F.N., Ramsey, L.W., Hill, G.J., MacQueen, P.J., Cornell, M.E., Robinson, E.L., "The Hobby-Eberly Telescope Completion Project", in *Large Ground-Based Telescopes*, Proc SPIE 4837, 919 (2003)

[2] Hill, G.J., MacQueen, P.J., Shetrone, M.D., & Booth, J.A., "Present and future instrumentation for the Hobby-Eberly Telescope", Proc. SPIE, 6269-5 (2006)

[3] Hill, G.J., MacQueen, P.J., Palunas, P., Barnes, S.I., Shetrone, M.D., "Present and future instrumentation for the Hobby-Eberly Telescope", Proc. SPIE, 7014-5 (2008)

[4] Savage, R., et al., "Current Status of the Hobby-Eberly Telescope wide field upgrade," *Proc. SPIE*, 7733-149 (2010)

[5] Hill, G.J., *et al*., "Current status of the Hobby-Eberly Telescope wide field upgrade," *Proc. SPIE*, 8444-19 (2012)

[6] Hill, G.J., Drory, N., Good, J., Lee, H., Vattiat, B.L., Kriel, H., Bryant, R., Elliot, L., Landiau, M., Leck, R., Perry, D., Ramsey, J., Savage, R., Damm, G., Fowler, J., Gebhardt, K., MacQueen, P.J., Martin, J., Ramsey, L.W., Shetrone, M., Schroeder, E., Cornell, M.E., Booth, J.A., and Moriera, W., "Deployment of the Hobby-Eberly Telescope Wide Field Upgrade", Proc. SPIE, 9145-5 (2014)

[7] Buckley, D.A.H., Swart, G.P., Meiring, J.G., "Completion of the Southern African Large Telescope", *Proc. SPIE*, 6267-19 (2006)

[8] Hill, G.J., MacQueen, P.J., Smith, M.P., Tufts, J.R., Roth, M.M., Kelz, A., Adams, J.J., Drory, N., Barnes, S.I., Blanc, G.A., Murphy, J.D., Gebhardt, K., Altmann, W., Wesley, G.L., Segura, P.R., Good, J.M., Booth, J.A., Bauer, S.-M., Goertz, J.A., Edmonston, R.D., Wilkinson, C.P., "Design, construction, and performance of VIRUS-P: the prototype of a highly replicated integral-field spectrograph for HET", *Proc. SPIE*, 7014-257 (2008)

[9] Hill, G.J., Tuttle, S.E., Drory, N., Lee, H., Vattiat, B.L., DePoy, D.L., Marshall, J.L., Kelz, A., Haynes, D., Fabricius, M., Gebhardt, K., Allen, R.D., Blanc, G., Chonis, T.S., Cornell, M.E., Dalton, G., Good, J., Jahn, T., Kriel, H., Landriau, M., MacQueen, P.J., Murphy, J.D., Prochaska, T., Nicklas, H., Ramsey, J., Roth, M.M., Savage, R., Snigula, J., "VIRUS: production and deployment of a massively replicated fiber integral field spectrograph for the upgraded Hobby-Eberly Telescope", Proc. SPIE, 9147-25 (2014)

[10] Hill, G.J., Tuttle, S.E., Vattiat, B.L., Lee, H., Drory, N., Kelz, A., Ramsey, J., DePoy, D.L., Marshall, J.L., Gebhardt, K., Chonis, T.S., Dalton, G.B., Farrow, D., Good, J.M., Haynes, D.M., Indahl, B.L., Jahn, T., Kriel, H., Montesano, F., Nicklas, H., Noyola, E., Prochaska, T., Allen, R.D., Blanc, G., Fabricius, M.H., Landriau, M., MacQueen, P.J., Roth, M.M., Savage, R., Snigula, J.M., "VIRUS: first deployment of the massively replicated fiber integral field spectrograph for the upgraded Hobby-Eberly Telescope", Proc. SPIE, 9908-54 (2016)

[11] Hill, G.J., "HETDEX and VIRUS: Panoramic Integral Field Spectroscopy with 35k fibres" in 'Multi-Object Spectroscopy in the Next Decade' a conference held in La Palma, March 2015, (eds. I. Skillen, M. Balcells & S. Trager), ASP Conference Series, in press (2016)

[12] Hill, G.J., Gebhardt, K., Komatsu, E., Drory, N., MacQueen, P.J., Adams, J.A., Blanc, G.A., Koehler, R., Rafal, Roth, M.M., Kelz, A., Grupp, F., Murphy, J., Palunas, P., Gronwall, C., Ciardullo, R., Bender, R., Hopp, U., and Schneider, D.P., "The Hobby-Eberly Telescope Dark Energy Experiment (HETDEX): Description and Early Pilot Survey Results", in Panoramic Views of the Universe, ASP Conf. Series, 399, 115 (2008)

[13] Burge, J.H., Benjamin, S.D., Dubin, M.B., Manuel, S.M., Novak, M.J. Oh, C.J., Valente, M.J., Zhao, C., Booth, J.A., Good, J.M., Hill, G.J., Lee, H., MacQueen, P.J., Rafal, M.D., Savage, R.D., Smith, M.P., Vattiat, B.L., "Development of a wide-field spherical aberration corrector for the Hobby Eberly Telescope", Proc. SPIE, 7733-51 (2010)

[14] Oh, C.-J., Frater, E., Zhao, C., Burge, J.H., "System alignment and performance test of a wide field corrector for the Hobby-Eberly telescope", Proc. SPIE, 9145-8 (2014)

[15] Lee, H., Hill, G.J., Good, J.M., Vattiat, B.L., Shetrone, M., Martin, J., Schroeder Mrozinski, E., Kriel, H., Oh, C.-J., Frater, E., Smith, B., Burge, J.H., "Delivery, installation, on-sky verification of Hobby Eberly Telescope wide-field corrector," Proc. SPIE 9906-156 (2016)
[16] Good, J.M., Hill, G.J., Leck, R.L., Landriau, M., Drory, N., Fowler, J.R., Kriel, H., Cornell, M.E., Booth, J.A., Lee, H., Savage, R., "Laboratory Performance Testing, Installation, and Commissioning of the Wide Field Upgrade Tracker for the Hobby-Eberly Telescope", Proc. SPIE, 9145-156 (2014)
[17] Good, J.M., Hill, G.J., Landriau, M., Lee, H., Schroeder-Mrozinski, E., Martin, J., Kriel, H., Shetrone, M., Fowler, J., Savage, R., Leck, R., "HET Wide Field Upgrade Tracker System Performance", Proc. SPIE 9906-167 (2016)
[18] Vattiat, B.L., et al., "Design, testing, and performance of the Hobby Eberly Telescope prime focus instrument package," Proc. SPIE, 8446-269 (2012)
[19] Vattiat, B.L., Hill, G.J., Lee, H., Moreira, W., Drory, N., Ramsey, J., Elliot, L., Landriau, M., Perry, D.M., Savage, R., Kriel, H., Haeuser, M., Mangold, F., "Design, alignment, and deployment of the Hobby Eberly Telescope prime focus instrument package", Proc. SPIE, 9147-172 (2014)
[20] Lee, H., et al., "Analysis of active alignment control of the Hobby-Eberly Telescope wide field corrector using Shack-Hartmann wavefront sensors," Proc. SPIE, 7738-18 (2010)
[21] Lee, H., et al., "Metrology systems for the active alignment control of the Hobby-Eberly Telescope wide-field upgrade," Proc. SPIE, 7739-28 (2010)
[22] Lee, H., et al., "Metrology systems of Hobby-Eberly Telescope wide field upgrade," Proc. SPIE, 8444-181 (2012)
[23] Chonis, T.S., Hill, G.J., Lee, H., Tuttle, S.E., Vattiat, B.L., Drory, N., Indahl, B.L., Peterson, T.W., Ramsey, J., "LRS2 – design, assembly, testing, and commissioning of the second generation low resolution spectrograph for the Hobby-Eberly Telescope", Proc. SPIE 9908-163 (2016)
[24] Worthington M., et al., "Design of VIRUS spectrograph support structure for the Hobby-Eberly Telescope dark energy experiment (HETDEX)," Proc. SPIE, 8444-213 (2012)
[25] Mollison, N.T., et al., "Design and development of a long-travel positioning actuator and tandem constant force actuator safety system for the Hobby-Eberly Telescope wide field upgrade," Proc. SPIE, 7733-150 (2010)
[26] Zierer, Jr., J.J., Wedeking, G.A., Beno, J.H., Good, J.M., "Design, testing, and installation of a high-precision hexapod for the Hobby-Eberly Telescope dark energy experiment (HETDEX)," Proc. SPIE, 8444-176 (2012)
[27] Worthington, M.S., et al., "Design and development of a high-precision, high-payload telescope dual-drive system," Proc. SPIE, 7733-201 (2010)
[28] Soukup I.M., et al., "Testing, characterization, and control of a multi-axis, high precision drive system for the Hobby-Eberly Telescope Wide Field Upgrade," Proc. SPIE, 8444-147 (2012)
[29] Beno, J.H., *et al*., "HETDEX tracker control system design and implementation," Proc. SPIE, **8444**-211 (2012)
[30] Ramsey, J., Drory, N., Bryant, R., Elliott, L., Fowler, J., Hill, G. J., Landriau, M., Leck, R., Vattiat, B., "A control system framework for the Hobby-Eberly Telescope", Proc. SPIE, 9913-160 (2016)
[31] Good, J.M., Lee, H., Hill, G.J., Vattiat, B.L., Perry, D., Kriel, H., Savage, R., "Design and Implementation of Coating Hardware for the Hobby-Ebberly Telescope Wide Field Corrector", Proc. SPIE, 9145-160 (2014)
[32] John M. Good, Gary J. Hill, Emily Schroeder-Mrozinski, Richard Savage, Herman Kriel, Scott Benjamin, Robert Stone, "Performance of Cable Isolators in the Transport of Large Optical Assemblies", Proc. SPIE 9906-14 (2016)
[33] Kelz, A., Jahn, T., Haynes, D.M., Hill, G.J., Murphy, J.D., Rutowska, M., Streicher, O., Neumann, J., Nicklas, N., Sandin, C., Fabricius, M., "HETDEX / VIRUS: testing and performance of 33,000 optical fibres", Proc. SPIE, 9147-269 (2014)
[34] Kelz, A., Jahn, T., Hill, G. J., Tuttle, S. E., Vattiat, B. L., Bauer, S. M. et al., "Commissioning of VIRUS integral-field units at the Hobby-Eberly Telescope", Proc. SPIE, 9908-319 (2016)
[35] Hill, G.J., Kelz, A., Murphy, J.D., Jahn, T., Haynes, D., Lee, H., Vattiat, B.L., M-Bauer, S., Drory, N., Tuttle, S.E., Neumann, J., Nicklas, H., Anwad, H., Fabricius, M.H., Montesano, F., Rutowska, M., Savage, R.D., Gebhardt, K., Roth, M.M., "The VIRUS 35k fiber system: design, fabrication, and characterization", Proceedings of *Fiber Optics in Astronomy IV*, PASP, submitted (2016)
[36] Lee, H., Hill, G.J., Vattiat, B.L., Smith, M.P., Haeuser, M., "Facility calibration unit of Hobby Eberly Telescope wide field upgrade," Proc. SPIE, 8444-172 (2012)
[37] Prochaska, T., Allen, R., Rheault, J. P., Cook, E., Baker, D., DePoy, D. L., Marshall, J. L., Hill, G., Perry, D., "VIRUS instrument enclosures," Proc. SPIE 9147-257 (2014)
[38] Smith, M.P., Mulholland, G.T., Booth, J.A., Good, J.M., Hill, G.J., MacQueen, P.J., Rafal, M.D., Savage, R.D., Vattiat, B.L., "The cryogenic system for the VIRUS array of spectrographs on the Hobby Eberly Telescope", Proc. SPIE, 7018-117 (2008)

[39] Chonis, T.S., et al., “Development of a cryogenic system for the VIRUS array of 150 spectrographs for the Hobby-Eberly Telescope,” Proc. SPIE, 7735-265 (2010)
[40] MacQueen, P.J., South, B.J., Strubhar, J.L., Wesley, G.L., Odoms, P.S. Edmonston, R.D., “The Hobby Eberly Telescope high resolution spectrograph upgrade”, Proc. SPIE, 9908-42 (2016)
[41] Mahadevan, S., Anderson, T., Bender, C., Halverson, S., Hearty, F., Levi, E., YLi, Y., Monson, A., Nelson, M., Ramsey, L., Robertson, P., Roy, A., Schwab, C., Kári Stefánsson, G., Terrien, R., “The habitable-zone planet finder: AI&V status and summary of research and development to achieve high precision NIR Doppler radial velocities”, Proc SPIE, 9908-40 (2016)